Chapter

Inhibition of Protein Fibrillation by Hydrogen Sulfide[1]

Manuel F. Rosario-Alomar, Tatiana Quiñones-Ruiz, Dmitry Kurouski, Valentin Sereda, Eduardo DeBarros-Ferreira, Lorraine De Jesús-Kim, Samuel Hernández-Rivera, Dmitri V. Zagorevski, Leishla M. Cruz-Collazo, Igor K. Lednev and Juan López-Garriga

Abstract

Amyloid fibrils are misfolded proteins, which are often associated with various neurodegenerative diseases such as Alzheimer's. The amount of hydrogen sulfide (H_2S) is known to be reduced in the brain tissue of people diagnosed with Alzheimer's disease relative to that of healthy individuals. Hen Egg-White Lysozyme (HEWL) forms typical β-sheet-rich fibrils during 70 minutes at low pH and high temperatures. These results are consistent with the ThT findings that β-sheets structure is also present in myoglobin (Mb), and hemoglobin (Hb) in the presence of 45% TFE. The addition of H_2S in the process completely inhibits the formation of amyloid fibrils in HEWL, Mb, and Hb as revealed by several spectroscopic techniques. Non-resonance Raman bands corresponding to disulfide (RSSR) vibrational modes in the 550-500 cm^{-1} spectral range decreases in intensity and is accompanied by the appearance of a new 490 cm^{-1} band assigned to the trisulfide group (RSSSR). Intrinsic tryptophan fluorescence shows a partial denaturation of HEWL containing trisulfide bonds. Overall, the Mb and Hb result ties excellent with the HEWL data showing that the presence of H_2S during these proteins fibrillation processes protects the α-helical protein structures, preventing the formation of amyloids in these different proteins moieties.

Keywords: hydrogen sulfide, amyloid fibril, protein aggregates, lysozyme, myoglobin, hemoglobin, Raman spectroscopy, ultraviolet Raman spectroscopy, unordered protein, disulfide, trisulfide

[1] Materials in this chapter related to the lysozyme fibrillation and its inhibition by H2S, including text and figures was previously published in Journal of Physical Chemistry. 2015;119:1265-1274. PMID: 2554579. The direct link to the article is https://pubs.acs.org/doi/10.1021/jp508471v. Any further permissions related to the related material should be directed to the ACS.

1. Introduction

Amyloids are large aggregates of misfolded proteins with a highly stable cross β-structure, which are associated with a variety of degenerative illnesses such as Alzheimer's, Parkinson's, and Huntington's diseases [1–3]. Proteins with different functionalities and native structures ranging from α-helical and β-sheet rich to intrinsically unordered are able to form amyloid fibrils *in vitro* with a characteristic cross-β core structure [4–6]. This observation leads to the conclusion that protein fibrillation is a generic property of a polypeptide chain. There are numerous research reports demonstrating that a general fibrillation mechanism involves a partially unfolded protein as the first intermediate state [7, 8]. Steps to follow include the formation of small aggregates and a β-sheet rich nucleus, which generates further protein aggregation and the formation of mature fibrils.

A reduced amount of hydrogen sulfide (H_2S) in the brain tissue of patients with Alzheimer's disease has been recently reported [9]. For centuries, people have been interested in H_2S for its role as a poisonous chemical. At high concentrations, H_2S inhibits cytochrome c and, as a consequence, the electron transport chain [10]. It also binds to hemoglobin forming a sulfhemoglobin complex as detected during sulfhemoglobinemia [11]. More recently, it has been demonstrated that H_2S has gasotransmitter functions, similar to CO and NO [12]. For example, a suspended animation-like state in mice has been achieved by administering ppm-levels of H_2S at low temperatures. The metabolic rate and body core temperature decrease and fully recover after such exposure, a promising medical benefit that reduces physiological damage after trauma [13]. In the last two decades, significant attention has been paid to understand the physiological role of H_2S and its endogenous production. H_2S is biosynthesized in mammalian tissue by non-enzymatic reactions and by the enzymatic degradation of cysteine by cystathionine β synthase (CBS), cystathionine γ lyase (CSE), cysteine aminotransferase (CAT), and cysteine lyase (CL) [14]. Consumption of garlic induces non-enzymatic H_2S production [15]. Moreover, aged garlic extract has been shown to cause a reduction of *in vivo* Aβ fibrils and soluble amyloid, as well as a decrease in tau conformational changes [16]. This indirect evidence concerning the role of H_2S in neurodegenerative diseases has motivated us to investigate the effects of H_2S on the formation of amyloid fibrils.

Small molecules can have a significant effect on the formation of amyloid fibrils. There is extensive literature on the inhibitory activity of various small molecules on protein fibrillation [17]. Recently, Arosio and coauthors have reviewed the development of amyloid inhibitors, such as antibodies and chaperones, small molecules (e.g., Congo red and polyphenols), colloidal inhibitors and organic/inorganic nanoparticles, as possible participants in the various states of protein aggregation [17–19]. These states include the inhibition of primary nucleation (monomer-to-oligomer transition), secondary nucleation (oligomer elongation), and postelongation. However, we have not found any published reports on the role of H_2S in protein aggregation.

It is well documented that H_2S reacts with disulfide bonds, leading one to hypothesize that this reaction could have a significant effect on the mechanism of protein fibrillation. Kumar and co-workers have reported that protecting disulfide bridges with iodoacetamide in an alkaline solution limits the lysozyme fibril growth to 50% [20]. This group has concluded that changing the dynamics of disulfide to *aberrant* disulfide bonds would redirect the process toward the formation of native-like lysozyme aggregates [20]. It has been reported that treating antibodies with H_2S has resulted in SS bond modifications, including the formation of trisulfide bonds (SSS) [21]. Surprisingly, no changes in antibody stability and function have been observed. H_2S can be incorporated as a sulfane sulfur, a divalent sulfur with six valence electrons, and an oxidation number of zero (S^0) that only binds to other sulfur atoms to form polysulfides [22]. Several research groups have also reported that the sulfur atom of

H_2S can be endogenously incorporated into a large amount of proteins by sulfuration, also known as sulfhydration of cysteines. This leads to the formation of protein persulfides (SSH), which could play an intermediary role in protein SSS formation [23].

Here, we have investigated the effect of H_2S on the aggregation of lysozyme, a glycoside hydroxylase responsible for antimicrobial protection in most mammalian species. HEWL is a single chain protein stabilized by four SS bonds in positions cys6-cys127, cys30-cys115, cys64-cys80, and cys76-cys94 [24]. It was found that H_2S inhibits the formation of HEWL fibrils. The effect of H_2S has been investigated under typical fibrillation conditions such as high temperature and acidic pH using DUVRR and non-resonance Raman spectroscopy, fluorescence, and atomic force microscopy (AFM). We have shown that in the presence of H_2S, HEWL forms spherical aggregates of unordered protein under fibrillation conditions. Cytotoxicity tests reveal that these spherical aggregates have no cell toxicity by contrast with typical HEWL fibrils. Our spectroscopic results, buttressed by data that has been published, indicate that H_2S reacts with protein disulfide bonds to form trisulfide bridges. This reaction results in significant lysozyme denaturation and the formation of spherical aggregates of unordered proteins, which prevent protein fibrillation.

However, because myoglobin (Mb) and hemoglobin (Hb) do not have any cysteine chemical bond, we pursued the effect of H_2S on the fibril formation of these vital hemeproteins. Mb and Hb are the most studied hemeproteins, because of their biological significance of oxygen binding. The role of Mb and Hb in the body is so important that the minimal unbalance of normal physiology can lead to toxicity and to cascade of reactions generating harmful products. For example, free radical formation in these hemeproteins unavoidably leads to oxidative damage of the heme and amino acids [25]. Also in certain circumstances, Mb and Hb isolated from their cellular environment may crosslink leading to kidney dysfunction, rhabdomyolysis, coma, and subarachnoid brain hemorrhage [26]. Other maladies include heme loss (hemophilia, hemolytic anemia), hemoglobinopathies (thalassemia [α and β], methemoglobinemia, posttranslational alterations), cardiovascular, and renal diseases [27–31]. Likewise, hemoglobin can protagonist sickle cell anemia where a mutation at the β6 position of Hb (β6Glu → Val) results in the polymerization of deoxy-sickle cell Hb (HbS) and subsequent aggregation into long fibers with amyloid-like structures [32, 33]. Regarding this, it has been shown that Hb under physiological conditions and in the presence of 45% 2,2,2-trifluoethanol (TFE) produces amyloid-like fibril structures. This observation was supported by ThT fluorescence, CD, and FTIR suggesting that Hb β-sheet conformation leads to Hb fibril formation [28]. The mechanism surrounding these fibril events remain almost unknown. Interestingly, our results also show that H_2S inhibits the fibril formation in both myoglobin and hemoglobin under physiological conditions and 45% TFE concentration and that increasing concentration of H_2S inhibits β-sheet formation and predominates the α-helix structure. The findings demonstrate the same H_2S effect on to the fibrillation of Mb monomer and Hb tetramer. Overall, it is very interesting that hydrogen sulfide is able to avoid the formation of fibril derivative in lysozyme and myoglobin and hemoglobin being their structures completely different.

2. Materials and methodology

The following chemicals were purchased from Sigma-Aldrich (St. Louis, MO, USA): 99.7% acetic acid (695092), sodium chloride (NaCl) (S771-3), HEWL (L6876), hemoglobin bovine (H2500), myoglobin from horse skeletal muscle (M0630), 2,2,2-trifluoroethanol 99% (T63002), potassium chloride (P3911), potassium phosphate monobasic (P5655) and potassium phosphate dibasic (1551128),

sodium sulfide nonahydrate salt (208043), dipropyl disulfide (149225), and trisulfide (6028-61-1).

2.1 HEWL solution preparation

Lysozyme was dissolved (25 mg/mL) in 20% acetic acid and 100 mM NaCl at pH 2.0 and incubated at 60°C to form fibrils under initial (control) conditions. To study the effect of H_2S, sodium sulfide nonahydrate salt (12 mM) was added to the control solution in a molar ratio of 1:5 (HEWL:H_2S), prior to the temperature elevation.

2.2 Myoglobin and hemoglobin fibril preparation

Myoglobin and hemoglobin were dissolved (15 and 20 mg/mL, respectively) in 20 mM phosphate buffer at pH 7.4; samples of Mb and Hb solutions were mixed with 45% of 2,2,2-trifluoroethanol and incubated at 37°C for 24 hours to form the fibrils (control conditions). Another batch of samples was prepared with sodium sulfide nonahydrate salt (60–300 μM, 12 mM) under the same control conditions, to evaluate H_2S effect [28, 34].

2.3 Non-resonance Raman experiments

Powder samples of native and aggregated HEWL were prepared by drying the solutions under nitrogen at room temperature, which removed the acetic acid. Raman spectra (785-nm excitation) of HEWL powder samples and pure dipropyl di- and trisulfide liquids were recorded using a Renishaw inVia confocal Raman spectrometer equipped with a research grade Leica microscope and 50× objective (numerical aperture, 0.55). Five accumulations of 30 s each were collected for each sample in the range of 400–1800 cm^{-1}. Wire 4.0 software was used for data collection. A laser power of approximately 11.5 mW was used to avoid sample photo-degradation.

2.4 TCEP test for trisulfides

A reaction with tris(2-carboxyethyl)phosphine (TCEP) reducing agent was used as a test for trisulfides [35]. Hen egg white lysozyme (HEWL) in native and aggregated form was incubated at pH 2.0 and room temperature for 90 minutes in the presence of TCEP. The reaction products were analyzed using normal Raman spectroscopy. Powder samples of HEWL-aggregates incubated at different concentrations of TCEP were prepared for non-resonance Raman spectroscopic analysis by drying the corresponding solutions under a nitrogen flow.

2.5 Deep UV resonance Raman spectroscopy (DUVRR)

DUVRR spectra (199.7 nm excitation) of 25 mg/mL HEWL were collected using a home built instrument equipped with a CCD camera (Roper Scientific, Inc.) cooled in liquid nitrogen [36]. A spinning quartz NMR tube with a magnetic stirrer was used for sampling. Each spectrum recorded an average of 20 accumulations with 30 s acquisition time. GRAMS/AI 7.0 software (Thermo Galactic, Salem, NH) was used for data processing.

2.6 Tryptophan and ThT fluorescence

Fluorescence spectra were measured in a JobinYvon Fluoromax-3 spectrofluorometer (JobinYvon, Edison, NJ). Intrinsic tryptophan fluorescence of

25 mg/mL HEWL was measured in a 10-μm path length cell without dilutions. The UV absorption was <0.05 at an excitation wavelength of 295.5 nm. The excitation and emission slits were 0.5 and 5 nm, respectively. Three spectral accumulations were taken, and the spectra were averaged for each sample. HEWL fibrils formed after 90 minutes of incubation were also characterized using intrinsic tryptophan fluorescence. Fibrils were washed in acetic acid solution twice in a procedure which included sonication for 10 minutes, centrifugation for 4 minutes at 13,000 rpm, the removal of supernatant liquid and re-suspension in an acetic acid solution. Fluorescence dye thioflavin T (ThT) is one of the most used probes for identification and analysis in the formation of amyloid fibrils both *in vivo* and *in vitro*. Once ThT binds to β-sheet-rich amyloid fibril structures, there is a characteristic blue shift in the emission spectrum from 510 to 480 nm [37–39]. In the ThT fluorescence assay, aliquots of 25 mg/mL HEWL were diluted in a molar ratio of 1:10 (HEWL:thioflavin T (ThT) dye) to a final concentration of 2.5 mM ThT. The excitation and emission wavelengths were 450 and 480 nm, respectively. The excitation and emission slits were 5 nm. Three recorded spectra were averaged for each measurement. ThT fluorescence intensity of Mb and Hb was monitored during fibrillation experiment: λ_{ex} = 440 nm and λ_{em} = 480 nm. The final protein sample and ThT concentration were 10 and 10 μM, respectively [28]. Fluorescence was measured using Biotek Synergy 4 (multi-mode microplate reader) with a 96 well-plate in a continuous acquisition (kinetics mode), every 5 minutes for 20 hours with gently orbital shake. We examined the time-dependence of Mb and Hb amyloid-like structures by monitoring thioflavin T fluorescence (480 nm) enhancement under a pH = 7.4 and T = 37°.

2.7 Circular dichroism spectroscopy

Far-UV circular dichroism (CD) measurements of Hb and Mb samples were performed on a Jasco-815 spectropolarimeter. Each spectrum was the average of six scans. Three replicates for each time point of the kinetic experiment were analyzed. Spectra were acquired at 0.5-nm intervals with a 4-s integration time and a bandwidth of 1.0 nm. Mb and Hb were analyzed at a final concentration of 0.5 mg/mL. All measurements were performed under nitrogen flow. The results were expressed as the mean residue ellipticity. Data were corrected for buffer contributions [28, 40, 41].

2.8 Atomic force microscope

Aliquots of HEWL incubated at 60°C, pH 2.0, 100 mM NaCl were cooled to room temperature and deposited on freshly cleaved mica. After a few minutes of exposure, the mica surface was rinsed with MQ water and dried. AFM images were collected using the SmartSPM 1000 system (AIST-NT, Novato, CA). Images were acquired in the tapping mode using silicon cantilevers with a 10–25 nm tip curvature radius.

3. Results

3.1 Aggregation and structural rearrangements of lysozyme

To form fibrils, HEWL was incubated at 60°C in 20% acetic acid (pH 2.0) and 100 mM NaCl, from here on referred to as control conditions. The morphology of lysozyme aggregates formed in the course of incubation under the fibrillogenic

conditions and in the presence of H_2S was characterized by AFM. The presence of typical long rode-like fibrils was evident after 90 minutes of incubation under control conditions (**Figure 1A**). However, incubation of HEWL in the presence of H_2S resulted in the formation of spherical aggregates instead of fibrils, as evident from AFM images (**Figure 1B**).

ThT fluorescence is used often to monitor the formation of amyloid fibrils. ThT fluorescence intensity increased dramatically after 70 minutes of incubation of lysozyme under control conditions, indicating the formation of amyloid fibrils (**Figure 1C**). However, no increase in ThT fluorescence intensity was observed for the HEWL solution incubated with H_2S within 48 hours. We investigated changes in the lysozyme secondary structure during incubation with and without H_2S using deep UV resonance Raman (DUVRR) spectroscopy. DUVRR has been used to study structural rearrangements of HEWL at all stages of fibrillation [36, 45, 46]. The DUVRR spectrum of HEWL excited at 199.7 nm was mainly composed of the amide chromosphere and the aromatic amino acid (Phe and Tyr) contributions [47]. A noticeable increase in the intensity and sharpness of the Am I band (approximately 1672 cm^{-1}) indicated the appearance of β-sheets due to the formation of fibrils [36, 48–50]. The DUVRR spectrum of fibrillated lysozyme under control conditions confirmed the formation of β-sheets. The spectrum of HEWL after 30 minutes of incubation under control conditions (**Figure 1D**, red) is similar to that reported previously for HEWL fibrils [36]. However, the DUVRR spectrum of lysozyme

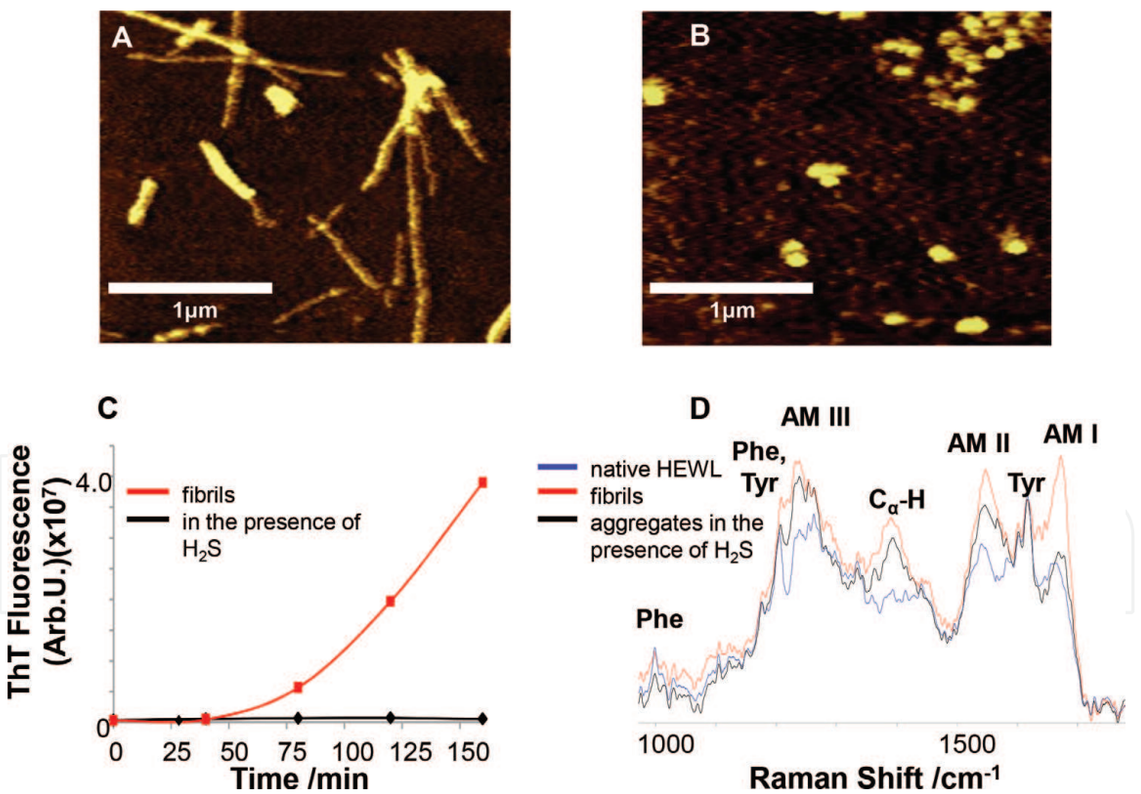

Figure 1.
Lysozyme forms β-sheet-rich fibrils under fibrillogenic control conditions and spherical aggregates of unordered protein under fibrillogenic conditions with H_2S incubation. AFM images of (A) HEWL fibrils formed after incubation of the control solution for 90 minutes and (B) HEWL aggregates formed after incubation of the solution in the presence of H_2S for 48 hours; scale bars are 1 μm. (C) Aggregation kinetics (ThT fluorescence) of HEWL incubated under control conditions (red) and in the presence of H_2S (black). (D) DUVRR spectra of native HEWL (blue), HEWL fibrils (red), and HEWL spherical aggregates (black) formed in the presence of H_2S; all spectra were normalized using the aromatic amino acid Raman band (approximately 1600 cm^{-1}) for comparison. The amide I vibrational mode (Am I) is dominated by C=O stretching, with minor contributions from C—N stretching and N—H bending [42]. Amide II (Am II) and amide III (Am III) bands involve significant C—N stretching, N—H bending, and C—C stretching [43]. The C_α—H bending vibrational mode involves C_α—H symmetric bending and C—C_α stretching [44].

incubated in the presence of H_2S confirmed the lack of β-sheet formation. In this case, the Am I band (approximately 1670 cm^{-1}) did not show a significant intensity change (**Figure 1D**, black). Instead, the Am I band shifted slightly to a higher frequency, signifying the formation of an unordered protein [36, 42]. This was further supported by the increase in C_α—H band intensity at 1390 cm^{-1} that was indicative of α-helix melting [51]. A significant change in Raman bands for Am III (approximately 1250 cm^{-1}) and Am II (approximately 1555 cm^{-1}) was consistent with the transition of α-helix to unordered protein. Therefore, AFM, ThT fluorescence, and DUVRR spectroscopy indicated the formation of unordered spherical aggregates of HEWL by contrast with β-sheet-rich fibrils in the presence of H_2S.

3.2 Intrinsic tryptophan fluorescence marker of the tertiary structural rearrangement

Tryptophan (Trp) fluorescence is an efficient intrinsic marker of local environments, which is often used for monitoring tertiary structural changes in proteins [47]. Native lysozyme at neutral pH shows a maximum Trp emission at 340 nm [52]. At pH 2.0 (20% acetic acid), the Trp fluorescence peak shifts to 345 nm, indicating a partial denaturation of lysozyme. A further minor shift to 347 nm due to HEWL fibril formation under control conditions was observed (**Figure 2B** and **C**). To confirm that the intrinsic Trp fluorescence is dominated by the signal from HEWL fibrils, the solutions (after incubation for 40 and 90 minutes) were sonicated, centrifuged, and re-suspended in 20% acetic acid to remove possible monomeric and oligomeric forms of the protein (**Figure 2B**). A significant shift of the Trp emission maximum, from 345 to 357 nm, was observed after 90 minutes of lysozyme incubation in the presence of H_2S (**Figure 2A** and **C**), with no further changes for at least 48 hours. This significant red shift is consistent with the previously reported maximum emission at 352 nm for fully denatured lysozyme in 6 M guanidinium-HCl at pH 7.0 [53]. Therefore, we conclude that incubation of lysozyme in the presence of H_2S results in a stronger denaturation than that which occurs during control fibrillation conditions.

3.3 Rearrangement of disulfide bonds

Non-resonance Raman spectroscopy of proteins offers a unique opportunity for characterizing the conformation of disulfide bridges [49]. The SS symmetric stretching vibrational mode is typically represented as a strong Raman band in the range of 505–550 cm^{-1} [49, 54]. The Raman spectrum of HEWL was found to change significantly in the SS signature region with incubation time (**Figure 3A**). A strong 507 cm^{-1} peak in the Raman spectrum of native HEWL represents the gauche-gauche-gauche (g-g-g) configuration of three SS bonds, and a small 523 cm^{-1} peak can be attributed to the gauche-gauche-trans (g-g-t) configuration of the fourth SS bond of lysozyme [49, 55]. The amplitudes of these peaks decreased, and a new peak appeared at 490 cm^{-1} as a result of HEWL incubation in the presence of 12 mM H_2S, indicating significant rearrangements of SS bonds (**Figure 3A**). The concentration of 12 mM H_2S corresponded to a 5:1 (H_2S:HEWL) molar ratio, chosen so that a sufficient number of H_2S molecules could react with all four lysozyme SS bonds assuming a 1:1 stoichiometric ratio. We are currently investigating the effect of H_2S concentrations. The 1003 cm^{-1} peak corresponding to phenylalanine was used to normalize Raman spectra in **Figure 3A** (region not shown). **Figure 3C** shows synchronous kinetic change in the area of the 507 and 490 cm^{-1} bands with incubation time up to 90 minutes [56]. No further changes were observed during 48 hours of additional incubation in the presence of H_2S

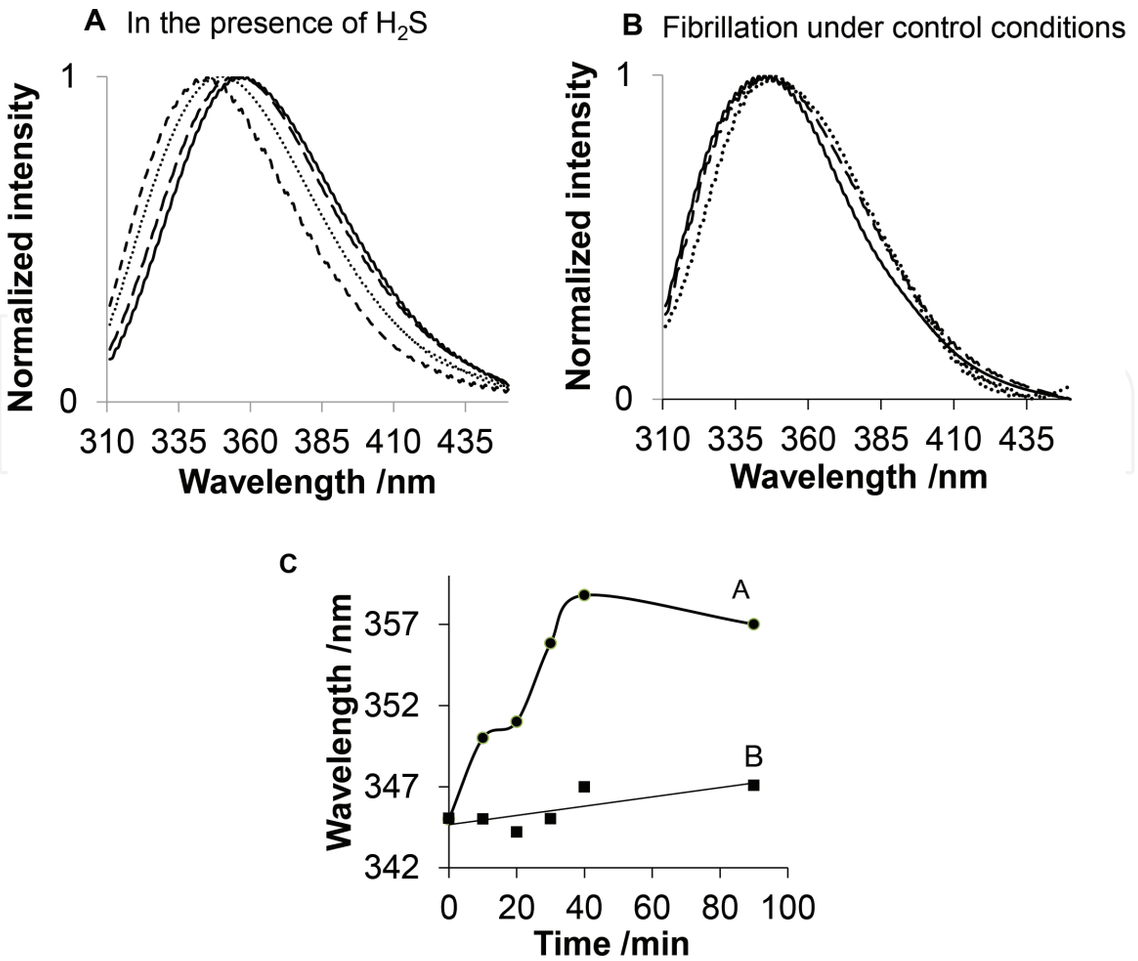

Figure 2.
Time dependent Trp fluorescence changes of lysozyme (A) incubated in the presence of H_2S for 0 minutes (dashes ---), 10 minutes (dots ...), 90 minutes (long dashes ---), 48 hours (solid line ___); (B) incubated with control solution for 0 minutes (solid line ___), 40 minutes (long dashes ---), and 90 minutes (dots ...); (C) Trp maximum emission wavelength of HEWL incubated with H_2S (A circles) and fibrillation under control conditions (B squares).

(data not shown). As discussed in detail below, dipropyl-trisulfide (DPTS) Raman spectrum contains a 485 cm^{-1} band (**Figure 3D**) characteristic to the trisulfide moiety that motivated us to investigate the possibility of assigning 490 cm^{-1} band in HEWL aggregate Raman spectrum to the SSS group. The non-resonance Raman spectroscopy of HEWL fibrillation under control conditions indicate that the 507 cm^{-1} peak does not change significantly during fibril formation (**Figure 3B**). Therefore, in the absence of H_2S, HEWL SS bands remain intact and the g-g-g conformation dominates, in agreement with our previous report [57].

3.4 Reduction of trisulfide bridges by TCEP

To test the hypothesis about the formation of trisulfide groups, we investigated the reaction of HEWL aggregates with TCEP reduction agent by normal Raman spectroscopy. TCEP reaction with SS groups is well known to result in oxidation of TCEP and formation of TCEP(O) and R-SH groups [58]. More recently, Cumnock et al. reported that TCEP reacted preferentially with SSS moieties in the presence of SS bridges until the majority of SSS groups were consumed according to Eqs. (1) and (2) [35]. SS bridges and thiophosphine TCEP(S) species are main products of TCEP-SSS reaction [35]. **Figure 4** shows Raman spectra of HEWL aggregates after incubation with different concentrations of TCEP (0.5, 1, 2.5, and 10 mM). The amount of aggregated HEWL molecules in these samples was kept about 3.0 mM.

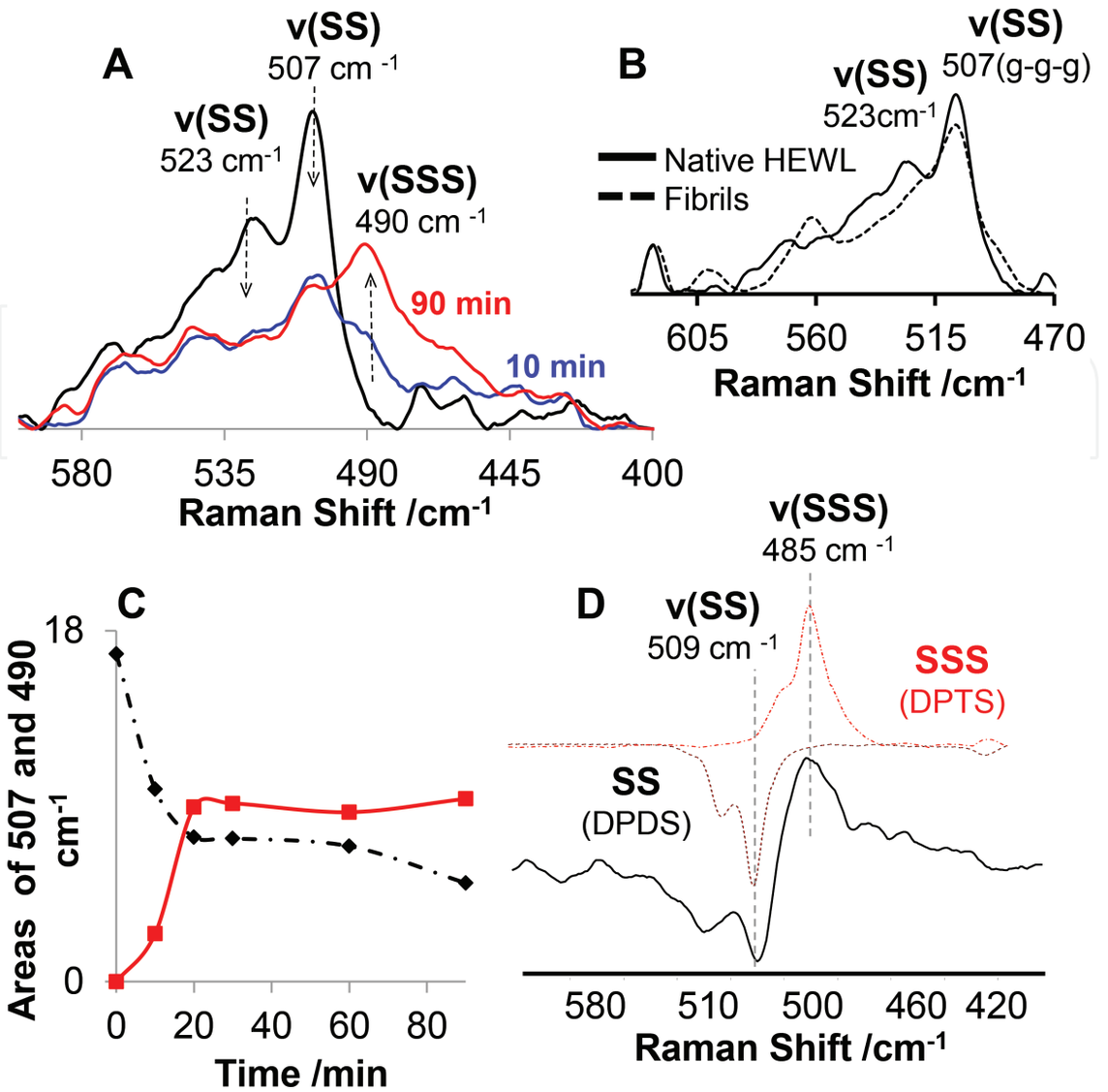

Figure 3.
Evolution of lysozyme disulfide bonds in the presence of H_2S probed by normal Raman spectroscopy. Raman spectra of HEWL incubated (A) in the presence of H_2S and (B) under control conditions, where 507 and 523 cm^{-1} bands correspond to g-g-g and g-g-t SS configurations, respectively. Synchronous kinetic change in the area of the 507 and 490 cm^{-1} bands is assigned to the newly formed RSSSR group. (C) The kinetics of RSSSR formation (490 cm^{-1}) and the decrease in the amount of RSSR (507 cm^{-1}) during the incubation of HEWL in the presence of H_2S. (D) The difference spectrum between normal Raman spectra of HEWL aggregated in the presence of H_2S acquired at 90- and 0-minute incubation [shown in (A), gray solid line]. The latter spectrum is represented by the expected spectral change demonstrating the disulfide-to-trisulfide transition symbolized by the inverted Raman spectrum of dipropyl disulfide (black dots and dash, -.-.-) and dipropyl trisulfide (red dots, ...).

$$TCEP + R - SSS - R \rightarrow TCEP(S) + R - SS - R \quad (1)$$

$$TCEP + R - SS - R \rightarrow TCEP(O) + 2\,R - SH \quad (2)$$

The Raman spectrum of HEWL aggregates was found to change significantly in the SSS/SS vibrational signature region with the addition of TCEP (**Figure 4A**). The SSS band at 490 cm^{-1} decreases after 0.5 mM TCEP addition that is in a good agreement with predominant reaction of TCEP with SSS groups. The amplitudes of both 490 and 507 cm^{-1} bands (SSS and SS, respectively) decreased as a result of HEWL incubation in the presence of higher concentration of TCEP (1–10 mM) indicating significant reduction of SS and SSS groups and formation of R-SH moiety in agreement with an increase in 2575 cm^{-1} band intensity (**Figure 4B**).

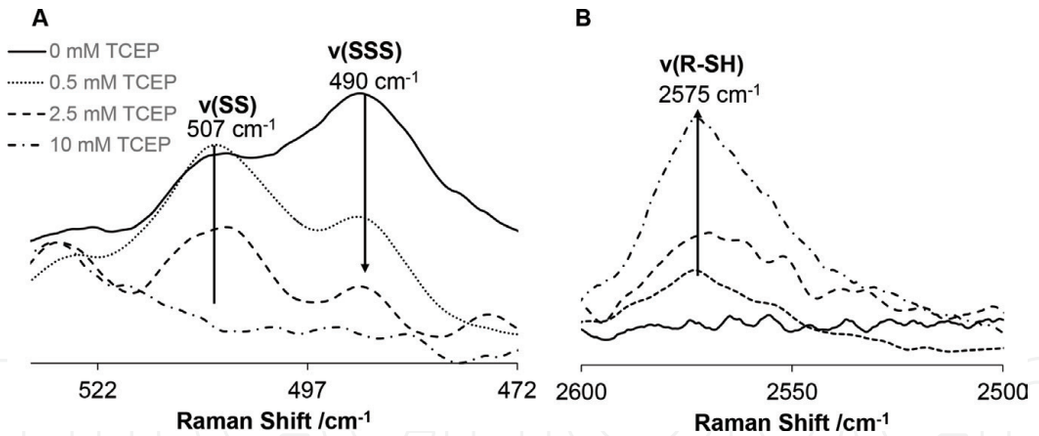

Figure 4.
Normal Raman spectra of HEWL aggregates in the presence of reducing agent TCEP with concentration 0 mM (solid line), 0.5 mM (dotted line), 1 mM (short dashed line), 2.5 mM (dashed line), and 10 mM (dashed dotted line). Selected spectral regions with characteristic Raman bands of disulfide and trisulfide moieties (A) as well as sulfhydryl (—SH) group (B) are shown. Phenylalanine Raman band at 1003 cm^{-1} was used to normalize the spectra (spectral region not shown).

3.5 Hydrogen sulfide inhibition of myoglobin and hemoglobin fibril formation

Figures 5A and **6A** demonstrate the formation of myoglobin and hemoglobin fibrils and its inhibition by hydrogen sulfide, respectively. The ThT fluorescence intensity associated to Mb and Hb amyloid fibrils (black) shows an initial lag process followed by a drastic increase as function of time. ThT fluorescence intensity is descriptive of prefibrillar oligomer intermediate species associated to the lag phase, while the positive slope is representative of fibrils with differing sizes and structures. Thus, the interaction of ThT with amyloid fibrils is highly specific, but neither amorphous aggregates nor soluble proteins in folded, unfolded, or partially folded states enhance ThT fluorescence [37–39]. Therefore, the data clearly show the existence of the myoglobin and hemoglobin amyloid fibril formation under the control condition of 2,2,2-trifluoroethanol (45%) and incubated at 37°C for

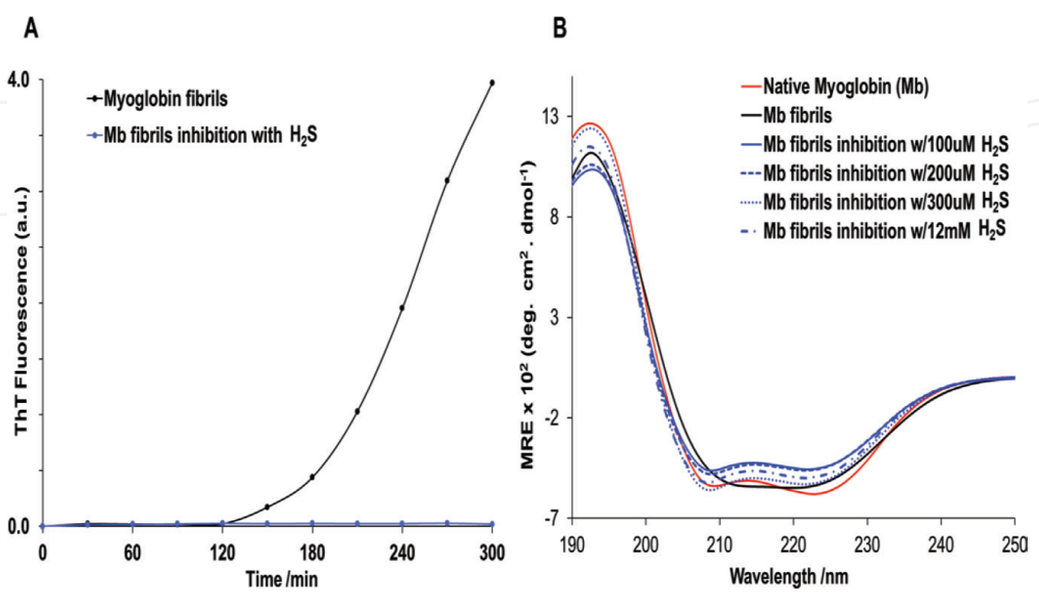

Figure 5.
Myoglobin fibrils and their inhibition by hydrogen sulfide. (A) Kinetics of myoglobin amyloid formation (black) and inhibition of Mb fibril formation (blue) in the presence of H_2S. (B) Far UV CD spectra of native Mb with a characteristic alpha-helical structure, Mb fibrils exhibiting beta-sheet structure, and Mb structures formed under the same condition of fibril formation, but in the presence of various H_2S (blue).

24 hours. There is a slightly difference between Mb and Hb lag phase leading to amyloid formation. However, when hydrogen sulfide is added under the control condition to Mb or Hb to generate fibrils, **Figures 5** and **6**, there is not an increase of ThT fluorescence (blue lines) for the duration of the experiment, independent of the lag phase difference between these hemeproteins. Therefore, the results demonstrate that under the experimental conditions, Mb and Hb fibrils are not observed in the presence of hydrogen sulfide. Curiously, a similar result was reported [34] for hen egg white lysozyme (HEWL), where the addition of H_2S in the fibril process completely inhibits the formation of β-sheet of amyloid fibrils.

Furthermore, **Figures 5B** and **6B** also show CD the spectra of native Mb and Hb with clear minima at 208 and 222 nm characteristic for α-helix conformation of protein (red line). These negative peaks at 208 and 222 nm result from $n \rightarrow \pi^*$ transition in the peptide bond of α-helical conformation [40, 41, 59, 60]. The presented results also indicate that both Mb and Hb form beta-sheet structures with a characteristic negative band near 218 nm and the positive band at 195 nm in CD spectra, which could be attributed to amyloid fibrils, in the presence of 45% of 2,2,2-trifluoroethanol (TFE) (black line). The data also collaborate analogous results indicating the formation of hemoglobin fibrils [28, 40, 41, 59, 60]. Nevertheless, when hydrogen sulfide is added, the CD spectra of both myoglobin and hemoglobin show 208 and 222 nm negative peaks typical for alpha-helical proteins (blue lines), suggesting the inhibition of fibrils by H_2S.

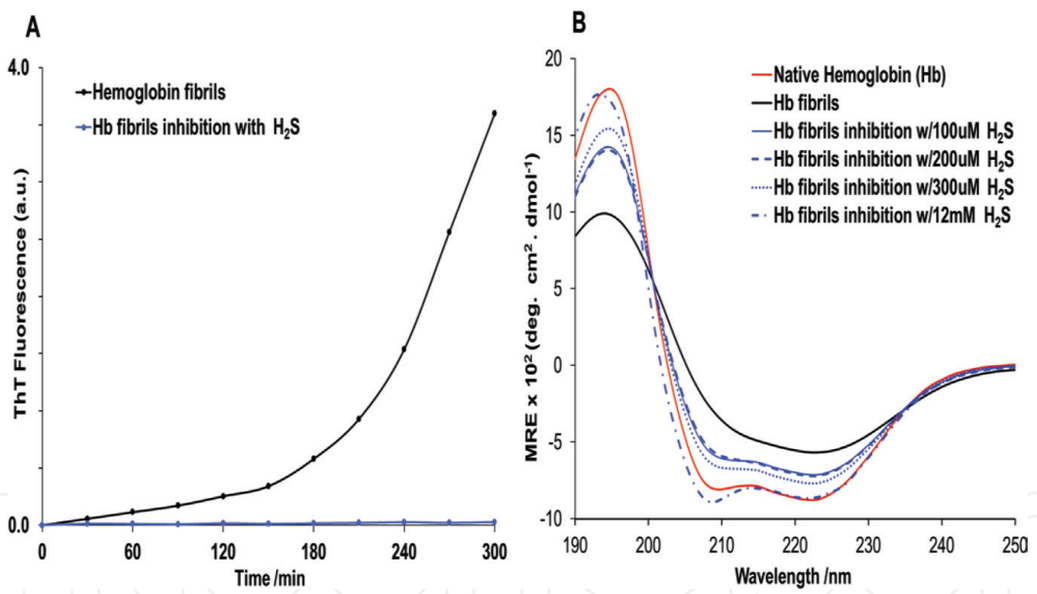

Figure 6.
Hemoglobin fibrils and their inhibition by hydrogen sulfide. (A) Kinetics of thioflavin T with hemoglobin amyloid formation (black) and in the presence of H_2S (blue). (B) Far-UV CD studies of native hemoglobin (red); hemoglobin fibrils inhibition in the presence of various concentrations of H_2S (blues) and hemoglobin fibrils (black).

4. Discussion

4.1 Evaluation of lysozyme secondary and tertiary structure

Lysozyme fibril formation has been extensively studied and characterized [36, 45, 61]. The most common methods used for studying the fibrillation process include AFM, ThT, and Trp fluorescence. DUVRR spectroscopy has been shown to be uniquely suitable for the structural characterization of proteins at all stages of the fibrillation process [51]. We utilized these complementary methods for

studying the effect of H_2S on the morphology and structure of lysozyme aggregates. Although fibril formation was not detected by AFM and ThT fluorescence assays, the intrinsic Trp fluorescence marker suggested that significant tertiary structure changes had taken place minutes after H_2S incubation began. The red shift of Trp fluorescence of greater than 10 nm is typical for unfolded lysozyme [36]. Changes were also evident for SS bridges at the same time scale, as discussed in the next section. The changes observed in the tryptophan local environment and in SS bonds indicate substantial changes in HEWL tertiary structure.

DUVRR spectroscopy was utilized to investigate changes in HEWL secondary structure during the incubation with and without H_2S. It was found that H_2S prevented the formation of β-sheet and resulted in a significant transition of α-helix to unordered protein. Moreover, we utilized DUVRR spectra of aggregated lysozyme to evaluate the protein secondary structure composition. Xu et al. have reported on the quantitative analysis of lysozyme DUVRR spectral changes during its denaturation [36]. According to that work, the amount of α-helix melting can be estimated from the intensity of C_α—H bending band. This band is conveniently isolated from other Raman bands. β-Sheet and unordered structures only contribute to C_α—H bending DUVRR band, while the α-helix does not make a noticeable input [51]. It is evident from amide I Raman bands in DUVRR spectra presented in **Figure 1D** that no fibril-type β-sheet is formed in HEWL aggregates since the Am I intensity does not increase. Therefore, the increase in the C_α—H band intensity in the spectrum of HEWL aggregates relative to that of native protein could be assigned to newly formed unordered structures. We normalized the DUVRR spectra of HEWL aggregates and native protein with the denatured-reduced HEWL spectrum reported by Xu et al. and estimated the amount of α-helix in HEWL aggregates as 11% [36]. Assuming that the amount of β-sheet in HEWL aggregates is approximately the same as in the native protein, we estimated the secondary structural composition of HEWL aggregates as 83% unordered, 11% α-helix, and 6% β-sheet.

To summarize the results concerning the significant tertiary structural rearrangements, α-helix melting, and lack of β-sheet formation, we conclude that H_2S causes more significant denaturation of lysozyme than that taking place during the initial stages of protein fibrillation, which is typically reported as *partial* protein denaturation [36]. We hypothesize that this significant lysozyme denaturation results in rapid protein aggregation, the formation of spherical species, and the prevention of the formation of β-sheets and fibrillation. In other words, H_2S redirects the process to "off-pathway" aggregation, preventing fibril formation [8, 62, 63]. This observation is consistent with an earlier report by Wang and colleagues, which demonstrated that fully denatured lysozyme forms amorphous aggregates that prevent fibril formation [64]. The protein has been fully denatured by reducing SS bonds with DTT_{red}. As a result, fully denatured lysozyme may lack the hydrophobic regions which are present in the partially unordered intermediates formed at the early stage of fibril formation. In addition, it is possible that amorphous aggregates decreased the effective concentration of HEWL available for fibril formation [64]. In agreement with Wang's report, our results suggest that lysozyme denatures strongly in the presence of H_2S and forms unordered aggregates that prevent β-sheet formation and fibrillation.

4.2 Formation of trisulfide bridges

According to **Figure 3**, the contributions of both g-g-g (507 cm^{-1} band) and g-g-t (523 cm^{-1} band) conformations of SS bonds to the Raman spectrum of HEWL decreased significantly during its incubation with H_2S. Simultaneously, a new peak

appeared at 490 cm^{-1} (**Figure 3A** and **C**). Nielsen and colleagues proposed that SSS bridges can form in proteins in the presence of H_2S via the thiol-disulfide exchange reaction, which is known to occur within cells [23]. We investigated the possibility of assigning a new Raman band at 490 cm^{-1} to the SSS moiety. Initially, we reproduced Raman spectra of two model compounds, dipropyl disulfide (DPDS) and dipropyl trisulfide (DPTS), shown in **Figure 3D**. In agreement with other published studies, these compounds exhibit strong Raman bands at 509 and 485 cm^{-1}, respectively, in agreement with the Raman spectra of native HEWL and HEWL spherical aggregates formed in the presence of H_2S [65, 66]. Furthermore, we obtained the difference spectrum by subtracting HEWL spectra after 0 and 90 minutes of incubation in the presence of H_2S and compared it to the expected spectral change representing the SS to SSS transition. The latter spectral change is depicted as a combination of dipropyl-disulfide and dipropyl-trisulfide spectra (**Figure 3D**). This spectral comparison provides further support for the hypothetical assignment of the 490 cm^{-1} Raman band to the SSS moiety.

Several studies have identified a 490 cm^{-1} Raman band in inorganic compounds and small organic molecules containing sulfur, and we report the appearance of this band in proteins for the first time [66–69]. Wieser and Krueger have assigned the 488 cm^{-1} Raman peak of H-SSS-H to a symmetric SS stretch with a contribution from the SSS bend [69]. Freeman has reported the Raman spectra of organic SS and SSS compounds, found in natural products where a strong 485 cm^{-1} stretching band has been observed in cyclic and acyclic trisulfides [66]. Janz et al. have reported Raman spectra of inorganic SSS from BaS_3 where 458 and 476 cm^{-1} bands were assigned to the symmetric stretching of SSS [68]. It is noteworthy that these frequencies can potentially be shifted in peptides. Kimbaris et al. have reported the Raman spectra of garlic oil, which contains a variety of compounds with SS and SSS groups [70]. We noticed an intense band at 489 cm^{-1} in these spectra that could potentially originate from an SSS moiety, although the assignment of the band was not discussed in the article. Overall, our hypothetical assignment of the 490 cm^{-1} Raman band to the SSS moiety is in agreement with data from the literature [66, 68]. The mechanism of SSS formation in proteins is unclear despite the significant interest that this topic has gained in recent years [21, 23, 35]. There is emerging evidence indicating that sulfane sulfur (S^0), which is generated from H_2S [56], is responsible for sulfuration through the formation of persulfide or trisulfide in proteins [71–73]. It would be interesting to investigate whether these SSS form by intra- or intermolecular processes. We are currently testing this hypothesis. It is noteworthy that the 490 cm^{-1} Raman band cannot be assigned to RSSH groups. These groups could form as a result of disulfide bond reduction in the presence of H_2S by a process known as sulfuration or sulfhydration [74].

4.3 The mechanism of HEWL, Mb, and Hb aggregation vs. fibrillation

Approximately 50% of all extracellular proteins have disulfide bridges [61]. SS bonds preserve the three dimensional structure of proteins and their cleavage typically results in significant disruption of the native conformations of proteins [57]. It is well established that SS bonds play a significant role in amyloid fibrillation [75]. Dobson and colleagues have reported that the reduction of SS bridges significantly accelerated the rate of human lysozyme aggregation [61]. It has also been demonstrated that reduction of four SS bonds to three bonds of apo-α-LA accelerates its fibrillation and leads to the formation of a new fibril polymorph with a different morphology and structure compared to fibrils formed from the wild-type LA [57]. At the same time, SS bonds of insulin remain intact and preserve their conformation during the fibrillation process [75]. Similar to insulin, the conformation of the SS

bonds in HEWL remains intact during the fibrillation of HEWL in control solution, as we have described here. It has been suggested that a partial denaturation of lysozyme precedes fibril formation because the native tertiary structure would not allow rearrangement to the cross-β sheet structure due to steric constraints [8, 76]. It has also been reported that partial denaturation, the first step of lysozyme fibrillation, is an irreversible process [46]. At the same time, a fully denatured lysozyme forms amorphous aggregates that prevent fibril formation [64]. It is believed that the fully denatured protein lacks the hydrophobic side chains present in partially unordered intermediates. In addition, amorphous aggregates potentially decrease the effective concentration of HEWL available for fibril formation [64]. In agreement with these observations, our results suggest that lysozyme denatures strongly in the presence of H_2S and forms unordered aggregates that prevent β-sheet formation and fibrillation.

Regarding this, it has been shown that Hb under physiological conditions and in presence of 45% 2,2,2-trifluoethanol (TFE) produces amyloid-like fibril species [28]. The mechanism surrounding these fibril events remains almost unknown. Curiously, myoglobin and hemoglobin do not have any S-S moiety in their chemical structures, and **Figures 5** and **6** show that the fibrillation inhibition effect of H_2S depends on its concentration. Specifically, the Mb and Hb α-helix assemblies are almost preserved at higher H_2S concentrations. Therefore, in these hemeproteins, it is not clear the inhibition mechanism by H_2S, since CD indicates that hydrogen sulfide prevents β-sheet formation and fibrillation without altering significantly the α-helical structure of Mb or Hb. Also similar to HEWL, the addition of H_2S to Mb or Hb fibrils does not revert the β-sheet amyloid fibrils to the native α-structure. These results are consistent with the ThT findings that β-sheets are present in Mb and Hb amyloid-like fibrils in the presence of 45% TFE and that increasing concentration of H_2S inhibits β-sheet formation. The findings demonstrate the same H_2S effect on to the fibrillation of Mb monomer and Hb tetramer, although some quantitative kinetic differences may be evident and need further study.

Acknowledgements

This work was supported in part by the National Science Foundation under Award CHE-1152752 (I.K.L.), NSF PREM: Wisconsin-Puerto Rico Partnership for Research and Education in Materials under Award DMR-0934115 (J.L.G), the National Institute of Health-INBRE PR under Award P20GM103475-13 (J.L.G.), the Alfred P. Sloan NACME Grant No. 2010-3-02, and BioXFEL-National Science Foundation Grant No. 1231306.

Abbreviations

H_2S	hydrogen sulfide
HEWL	hen egg white lysozyme
DUVRR	deep ultraviolet resonance Raman
AFM	atomic force microscopy
ThT	thioflavin T
cys	cysteine
SOD	super oxide dismutase
hGH	human growth hormone
DPDS	dipropyl disulfide
DPTS	dipropyl trisulfide
DTT	dithiothreitol

Mb	myoglobin
Hb	hemoglobin
TFE	2,2,2-trifluoroethanol
CD	circular dichroism spectroscopy

Author details

Manuel F. Rosario-Alomar[1†], Tatiana Quiñones-Ruiz[2†], Dmitry Kurouski[2], Valentin Sereda[2], Eduardo DeBarros-Ferreira[2], Lorraine De Jesús-Kim[3], Samuel Hernández-Rivera[1], Dmitri V. Zagorevski[4], Leishla M. Cruz-Collazo[1†], Igor K. Lednev[2] and Juan López-Garriga[1*]

1 Department of Chemistry, University of Puerto Rico at Mayagüez, Mayagüez, Puerto Rico

2 Department of Chemistry, University at Albany, Albany, NY, USA

3 Department of Biology, University of Puerto Rico at Mayagüez, Mayagüez, Puerto Rico

4 Center for Biotechnology and Interdisciplinary Studies, Rensselaer Polytechnic Institute, Troy, NY, USA

*Address all correspondence to: juan.lopez16@upr.edu

† These authors contributed equally

References

[1] Serpell LC. Alzheimer's amyloid fibrils: Structure and assembly. Biochimica et Biophysica Acta-Molecular Basis of Disease. 2000;**1502**:16-30

[2] Conway KA, Harper JD, Lansbury PT Jr. Fibrils formed in vitro from alpha-synuclein and two mutant forms linked to Parkinson's disease are typical amyloid. The Biochemist. 2000;**39**:2552-2563

[3] Kantcheva RB, Mason R, Giorgini F. Aggregation-prone proteins modulate huntingtin inclusion body formation in yeast. PLoS Currents Huntington Disease. 2014;**6**:1-11

[4] Glenner GG. Amyloid deposits and amyloidosis. The beta-fibrilloses (first of two parts). The New England Journal of Medicine. 1980;**302**:1283-1292

[5] Blake C, Serpell L. Synchrotron X-ray studies suggest that the core of the transthyretin amyloid fibril is a continuous beta-sheet helix. Structure. 1996;**4**:989-998

[6] Lednev IK. Amyloid fibrils: The eighth wonder of the world in protein folding and aggregation. Biophysical Journal. 2014;**106**:1433-1435

[7] Uversky VN, Li J, Fink AL. Evidence for a partially folded intermediate in alpha-synuclein fibril formation. The Journal of Biological Chemistry. 2001;**276**:10737-10744

[8] Uversky VN, Fink AL. Conformational constraints for amyloid fibrillation: The importance of being unfolded. Biochimica et Biophysica Acta-Proteins Proteomics. 2004;**1698**:131-153

[9] Eto K, Asada T, Arima K, Makifuchi T, Kimura H. Brain hydrogen sulfide is severely decreased in Alzheimer's disease. Biochemical and Biophysical Research Communications. 2002;**293**:1485-1488

[10] Wang R. Physiological implications of hydrogen sulfide: A whiff exploration that blossomed. Physiological Reviews. 2012;**92**:791-896

[11] Pietri R, Roman-Morales E, Lopez-Garriga J. Hydrogen sulfide and hemeproteins: Knowledge and mysteries. Antioxidants & Redox Signaling. 2011;**15**:393-404

[12] Fukuto JM, Carrington SJ, Tantillo DJ, Harrison JG, Ignarro LJ, Freeman BA, et al. Small molecule Signaling agents: The integrated chemistry and biochemistry of nitrogen oxides, oxides of carbon, dioxygen, hydrogen sulfide, and their derived species. Chemical Research in Toxicology. 2012;**25**:769-793

[13] Blackstone E, Morrison M, Roth MB. H_2S induces a suspended animation-like state in mice. Science. 2005;**308**:518

[14] Li L, Rose P, Moore PK. Hydrogen sulfide and cell signaling. Annual Review of Pharmacology and Toxicology. 2011;**51**:169-187

[15] Benavides GA, Squadrito GL, Mills RW, Patel HD, Isbell TS, Patel RP, et al. Hydrogen sulfide mediates the vasoactivity of garlic. Proceedings of the National Academy of Sciences of the United States of America. 2007;**104**:17977-17982

[16] Chauhan NB. Effect of aged garlic extract on APP processing and tau phosphorylation in Alzheimer's transgenic model Tg2576. Journal of Ethnopharmacology. 2006;**108**:385-394

[17] Arosio P, Vendruscolo M, Dobson CM, Knowles TPJ. Chemical kinetics for drug discovery to

combat protein aggregation diseases. Trends in Pharmacological Sciences. 2014;**35**:127-135

[18] Kayed R, Head E, Sarsoza F, Saing T, Cotman CW, Necula M, et al. Fibril specific, conformation dependent antibodies recognize a generic epitope common to amyloid fibrils and fibrillar oligomers that is absent in prefibrillar oligomers. Molecular Neurodegeneration. 2007;**2**:18

[19] Kurouski D, Luo H, Sereda V, Robb FT, Lednev IK. Rapid degradation kinetics of amyloid fibrils under mild conditions by an archaeal chaperonin. Biochemical and Biophysical Research Communications. 2012;**422**:97-102

[20] Ravi VK, Goel M, Kotamarthi HC, Ainavarapu SRK, Swaminathan R. Preventing disulfide bond formation weakens non-covalent forces among lysozyme aggregates. PLoS One. 2014;**9**:e87012

[21] Gu S, Wen D, Weinreb PH, Sun Y, Zhang L, Foley SF, et al. Characterization of trisulfide modification in antibodies. Analytical Biochemistry. 2010;**400**:89-98

[22] Ogasawara Y, Isoda S, Tanabe S. Tissue and subcellular distribution of bound and acid-labile sulfur, and the enzymic capacity for sulfide production in the rat. Biological & Pharmaceutical Bulletin. 1994;**17**:1535-1542

[23] Nielsen RW, Tachibana C, Hansen NE, Winther JR. Trisulfides in proteins. Antioxidants & Redox Signaling. 2011;**15**:67-75

[24] David C, Foley S, Enescu M. Protein S-S bridge reduction: A Raman and computational study of lysozyme interaction with TCEP. Physical Chemistry Chemical Physics. 2009;**11**:2532-2542

[25] Reeder B, Sharpe M, Kay A, Kerr M, Moore K, Wilson M. Toxicity of myoglobin and haemoglobin: Oxidative stress in patients with rhabdomyolysis and subarachnoid haemorrhage. Biochemical Society Transactions. 2002;**30**(4):745-748. DOI: 10.1042/bst0300745

[26] Reeder B. The redox activity of hemoglobins: From physiologic functions to pathologic mechanisms. Antioxidants and Redox Signaling. 2010;**13**(7):1087-1123. DOI: 10.1089/ars.2009.2974

[27] Sawicki K, Chang H, Ardehali H. Role of heme in cardiovascular physiology and disease. Journal of the American Heart Association. 2015;**4**(1):e001138. DOI: 10.1161/JAHA.114.001138

[28] Iram A, Naeem A. Detection and analysis of protofibrils and fibrils of hemoglobin: Implications for the pathogenesis and cure of heme loss related maladies. Archives of Biochemistry and Biophysics. 2013;**533**:69-78. DOI: 10.1016/j.abb.2013.02.019

[29] Forget B, Bunn H. Classification of the disorders of hemoglobin. Cold Spring Harbor Perspectives in Medicine. 2013;**3**:a011684. DOI: 10.1101/cshperspect.a011684

[30] Bilska-Wilkosz A, Iciek M, Górny M, Kowalczyk-Pachel D. The role of hemoproteins: Hemoglobin, myoglobin and neuroglobin in endogenous thiosulfate production processes. International Journal of Molecular Sciences. 2017;**18**:1315. DOI: 10.3390/ijms18061315

[31] Alayash A. Hemoglobin-based blood substitutes and the treatment of sickle cell disease: More harm than help? Biomolecules. 2017;**7**:2. DOI: 10.3390/biom7010002

[32] Garcia-Seisdedos H, Empereur-Mot C, Elad N, Levy E. Proteins evolve

on the edge of supramolecular self-assembly. Nature. 2017;**548**:244-247. DOI: 10.1038/nature23320

[33] Dykes G, Crepeau R, Edelstein S. Three-dimensional reconstruction of the 14-filament fibers of hemoglobin S. Journal of Molecular Biology. 1979;**130**(4):451-472. DOI: 10.1016/0022-2836(79)90434-0

[34] Rosario-Alomar M, Quiñones-Ruiz T, Kurouski D, Sereda V, Ferreira E, De Jesus-Kim L, et al. Hydrogen sulfide inhibits amyloid formation. The Journal of Physical Chemistry B. 2015;**119**: 1265-1274. DOI: 10.1021/jp508471v

[35] Cumnock K, Tully T, Cornell C, Hutchinson M, Gorrell J, Skidmore K, et al. Trisulfide modification impacts the reduction step in antibody-drug conjugation process. Bioconjugate Chemistry. 2013;**24**:1154-1160

[36] Xu M, Ermolenkov VV, Uversky VN, Lednev IK. Hen egg white lysozyme fibrillation: A deep-UV resonance Raman spectroscopic study. Journal of Biophotonics. 2008;**1**:215-229

[37] Gade Malmos K, Blancas-Mejia L, Weber B, Buchner J, Ramirez-Alvarado M, Naiki H, et al. ThT 101: A primer on the use of thioflavin T to investigate amyloid formation. Amyloid. 2017;**24**(1):1-16. DOI: 10.1080/13506129.2017.1304905

[38] Shoffner S, Schnell S. Estimation of the lag time in a subsequent monomer addition model for fibril elongation. Physical Chemistry Chemical Physics. 2016;**18**:21259. DOI: 10.1039/c5cp07845h

[39] Xue C, Lin TY, Chang D, Guo Z. Thioflavin T as an amyloid dye: Fibril quantification, optimal concentration and effect on aggregation. Royal Society Open Science. 2017;**4**:160696. DOI: 10.1098/rsos.160696

[40] Nasreen K, Ahamad S, Ahmad F, Hassan M, Islam A. Macromolecular crowding induces molten globule state in the native myoglobin at physiological pH. International Journal of Biological Macromolecules. 2018;**106**:130-139. DOI: 10.1016/j.ijbiomac.2017.08.014

[41] Grenfield NJ. Using circular dichroism spectra to estimate protein secondary structure. Nature Protocols. 2006;**1**(6):2876-2890. DOI: 10.1038/nprot.2006.202

[42] Copeland RA, Spiro TG. Ultraviolet resonance Raman spectra of cytochrome c conformational states. The Biochemist. 1985;**24**:4960-4968

[43] Myshakina NS, Asher SA. Peptide bond vibrational coupling. The Journal of Physical Chemistry B. 2007;**111**:4271-4279

[44] Wang Y, Purrello R, Jordan T, Spiro TG. UVRR spectroscopy of the peptide bond. 1. Amide S, a nonhelical structure marker, is a C.alpha.H bending mode. Journal of the American Chemical Society. 1991;**113**:6359-6368

[45] Xu M, Ermolenkov VV, He W, Uversky VN, Fredriksen L, Lednev IK. Lysozyme fibrillation: Deep UV Raman spectroscopic characterization of protein structural transformation. Biopolymers. 2005;**79**:58-61

[46] Xu M, Shashilov V, Lednev IK. Probing the cross-β core structure of amyloid fibrils by hydrogen-deuterium exchange deep ultraviolet resonance Raman spectroscopy. Journal of the American Chemical Society. 2007;**129**:11002-11003

[47] Lednev IK. Vibrational spectroscopy: Biological applications of ultraviolet Raman spectroscopy. In: Uversky VN, Permyakov EA, editors. Protein Structures, Methods in Protein Structures and Stability Analysis. New York: Nova Science Publishers, Inc.; 2007

[48] Asher SA, Ianoul A, Mix G, Boyden MN, Karnoup A, Diem M, et al. Dihedral ψ angle dependence of the amide III vibration: A uniquely sensitive UV resonance Raman secondary structural probe. Journal of the American Chemical Society. 2001;**123**:11775-11781

[49] Tu AT. Raman Spectroscopy in Biology: Principles and Applications. Wiley: University of California; 1982

[50] Lednev I, Ermolenkov V, He W, Xu M. Deep-UV Raman spectrometer tunable between 193 and 205 nm for structural characterization of proteins. Analytical and Bioanalytical Chemistry. 2005;**381**:431-437

[51] Oladepo SA, Xiong K, Hong Z, Asher SA, Handen J, Lednev IK. UV resonance Raman investigations of peptide and protein structure and dynamics. Chemical Reviews. 2012;**112**:2604-2628

[52] Imoto T, Forster LS, Rupley JA, Tanaka F. Fluorescence of lysozyme: Emissions from tryptophan residues 62 and 108 and energy migration. Proceedings of the National Academy of Sciences of the United States of America. 1972;**69**:1151-1155

[53] Pajot P. Fluorescence of proteins in 6-M guanidine hydrochloride. The FEBS Journal. 1976;**63**:263-269

[54] Van Wart HE, Lewis a, Scheraga HA, Saeva FD. Disulfide bond dihedral angles from Raman spectroscopy. Proceedings of the National Academy of Sciences of the United States of America. 1973;**70**:2619-2623

[55] Nakanishi M, Takesada H, Tsuboi M. Conformation of the cystine linkages in bovine α-lactalbumin as revealed by its Raman effect. Journal of Molecular Biology. 1974;**89**:241-243

[56] Kocherbitov V, Latynis J, Misiūnas A, Barauskas J, Niaura G. Hydration of lysozyme studied by Raman spectroscopy. Journal of the Chemical Society B. 2013;**117**:4981-4992

[57] Lednev DKAIK. The impact of protein disulfide bonds on the amyloid fibril morphology. International Journal of Nanoscience and Nanotechnology. 2011;**2**:167-176

[58] Burns JA, Butler JC, Moran J, Whitesides GM. Selective reduction of disulfides by tris(2-carboxyethyl) phosphine. The Journal of Organic Chemistry. 1991;**56**:2648-2650

[59] Chen T, Zhu S, Shang Y, Ge C, Jiang G. Binding of dihydromyricetin to human hemoglobin: Fluorescence and circular dichroism studies. Spectrochimica Acta Part A: Molecular and Biomolecular Spectroscopy. 2012;**93**:125-130. DOI: 10.1016/j.saa.2012.02.109

[60] Kelly SM, Jess TJ, Price NC. How to study proteins by circular dichroism. Biochimica et Biophysica Acta (BBA)-Proteins and Proteomics. 2005;**1751**(2):119-139. DOI: 10.1016/j.bbapap.2005.06.005

[61] Mossuto MF, Bolognesi B, Guixer B, Dhulesia A, Agostini F, Kumita JR, et al. Disulfide bonds reduce the toxicity of the amyloid fibrils formed by an extracellular protein. Angewandte Chemie International Edition in English. 2011;**50**:7048-7051

[62] Dobson CM. Protein folding and misfolding. Nature. 2003;**426**:884-890

[63] Powers ET, Powers DL. Mechanisms of protein fibril formation: Nucleated polymerization with competing off-pathway aggregation. Biophysical Journal. 2008;**94**:379-391

[64] Wang SS, Liu K-N, Wang B-W. Effects of dithiothreitol on the amyloid fibrillogenesis of hen egg-white lysozyme. The FBES Journal. 2010;**39**:1229-1242

[65] Sugeta H, Go A, Miyazawa T. Vibrational spectra and molecular conformations of dialkyl disulfides. Bulletin of the Chemical Society of Japan. 1973;**46**:3407-3411

[66] Freeman SK. Applications of laser Raman spectroscopy to natural products research. Journal of Agricultural and Food Chemistry. 1973;**21**:521-525

[67] Rebouças JS, Patrick BO, James BR. Thiol, disulfide, and trisulfide complexes of Ru porphyrins: Potential models for iron-sulfur bonds in heme proteins. Journal of the American Chemical Society. 2012;**134**:3555-3570

[68] Janz GJ, Roduner E, Coutts JW, Downey JR. Raman studies of sulfur-containing anions in inorganic polysulfides. Barium trisulfide. Inorganic Chemistry. 1976;**15**:1751-1754

[69] Wieser H, Krueger PJ, Muller E, Hyne JB. Vibrational spectra and a force field for H_2S3 and H_2S4. Canadian Journal of Chemistry. 1969;**47**:1633-1637

[70] Kimbaris AC, Siatis NG, Pappas CS, Tarantilis PA, Daferera DJ, Polissiou MG. Quantitative analysis of garlic (*Allium sativum*) oil unsaturated acyclic components using FT-Raman spectroscopy. Food Chemistry. 2006;**94**:287-295

[71] Toohey JI. Sulfur signaling: Is the agent sulfide or sulfane? Analytical Biochemistry. 2011;**413**:1-7

[72] Greiner R, Palinkas Z, Basell K, Becher D, Antelmann H, Nagy P, et al. Polysulfides link H_2S to protein thiol oxidation. Antioxidants & Redox Signaling. 2013;**19**:1749-1765

[73] Kimura H. The physiological role of hydrogen sulfide and beyond. Nitric Oxide. 2014;**41**:4-10

[74] Kabil O, Banerjee R. Redox biochemistry of hydrogen sulfide. The Journal of Biological Chemistry. 2010;**285**:21903-21907

[75] Kurouski D, Washington J, Ozbil M, Prabhakar R, Shekhtman A, Lednev IK. Disulfide bridges remain intact while native insulin converts into amyloid fibrils. PLoS One. 2012;**7**:e36989

[76] Booth DR, Sunde M, Bellotti V, Robinson CV, Hutchinson WL, Fraser PE, et al. Instability, unfolding and aggregation of human lysozyme variants underlying amyloid fibrillogenesis. Nature. 1997;**385**:787-793